

Production of an Office Stapler by Material Extrusion Process, using DfAM as Optimization Strategy

C. Oliveira¹, M. Maia², J. M. Costa³

¹Department of Metallurgical and Materials Engineering, Faculdade de Engenharia, Universidade do Porto, Rua Dr. Roberto Frias, 4200-465 PORTO, Portugal (up201706715@edu.fe.up.pt)

²Department of Metallurgical and Materials Engineering, Faculdade de Engenharia, Universidade do Porto, Rua Dr. Roberto Frias, 4200-465 PORTO, Portugal (up201706019@edu.fe.up.pt)




³Department of Metallurgical and Materials Engineering, Faculdade de Engenharia, Universidade do Porto and LAETA/INEGI - Institute of Science and Innovation in Mechanical and Industrial Engineering, Rua Dr. Roberto Frias, 4200-465 PORTO, Portugal (jose.costa@fe.up.pt). ORCID [0000-0002-1714-4671](https://orcid.org/0000-0002-1714-4671)

Abstract

For the last few decades, the rapid growth of Additive Manufacturing (AM) technologies has been seeable. It is expected to keep maturing continuously due to its advantages compared to conventional manufacturing technologies: flexibility, reliability, energy consumption, and material efficiency. This research article addresses the development and production of a stapler using the Material Extrusion AM process. It intends to show the development steps to redesign an everyday stapler, into an added-value tool, from the selection and fixture of the CAD model and generative design through Fusion 360 to its optimization on nTopology, simulation, and plot of the part in Eiger.

Author Keywords. Additive Manufacturing, Metallic Materials, Inconel 625, Fused Deposition Modelling, Fused Filament Fabrication, Stapler, Design for Additive Manufacturing, Additive Manufacturing Design Framework, *Fusion 360*, *nTopology*, *Eiger*.

Type: Research Article

 Open Access  Peer Reviewed  CC BY

1. Introduction

Valuing its benefits, when compared to conventional manufacturing processes, Additive Manufacturing (AM) is one of the most promising creations of the 20th century. It has grown, as a new market, ever since. According to the ASTM52921-13(2019) (ASTM 2019), AM is defined as the joining of materials to produce parts from tridimensional (3D) models, usually layer upon layer. The general AM procedure starts with a 3D CAD model, whose composition is feasible to be layer-on-layer. The raw material is deposited on a base, which moves after each layer is produced, keeping a constant height between the base and layer. A component with potentially complex geometrical characteristics is obtained and removed from the base bed (Tofail et al. 2018).

The Material Extrusion process (MEX) is also known as Fused Deposition Modeling (FDM) or Fused Filament Fabrication (FFF). It is one of the most widely used AM techniques for polymeric materials. It is becoming increasingly utilized in metallic and ceramic materials (Singh, Ramakrishna, and Singh 2017; Gonzalez-Gutierrez et al. 2018), as it allows the production of parts with complex geometries. Nevertheless, its use remains behind Powder Bed Fusion in industrial contexts, as MEX is still a rapid prototyping tool. In this technique, a

temperature-controlled head extrudes the molten material through a thin nozzle onto a build platform. It is deposited layer-by-layer at predetermined locations, where it cools and solidifies, as shown in [Figure 1](#) (Costa et al. 2021). When a layer is finished, the building platform moves down, allowing the deposition of a new one, and this process is repeated until the piece is completed. The metal chosen is used to produce the component for the printing operations. In contrast, ceramics might be used as a release enabler from construction supports and build plate to support the structure during the removal. This way, additional steps of debinding and sintering treatments will be necessary. It requires debinding to remove polymeric additives used, which can be thermal or catalytic and sintering for an increment of strength by bonding the particles (Costa et al. 2021).

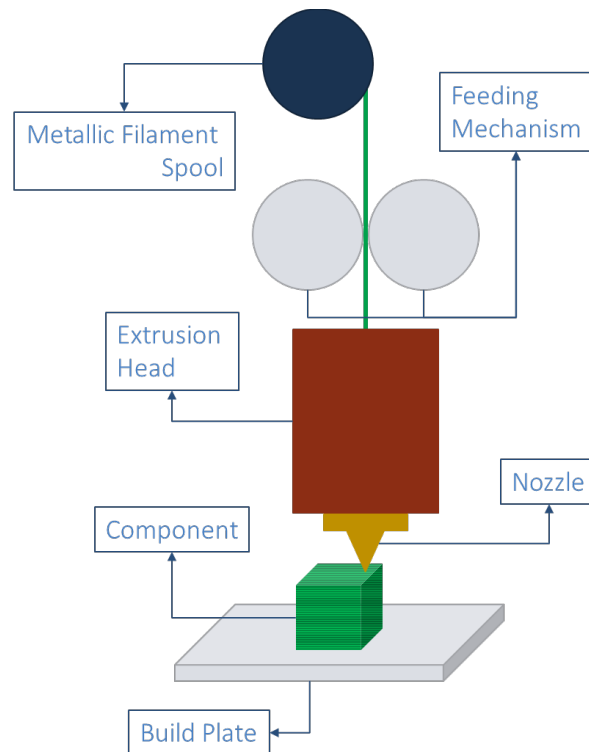


Figure 1: Schematics for Metal-Based ME Equipment (Costa et al. 2021).

MEX is one of the most cost-effective ways of producing custom-specific parts and prototypes, while the lead times are short. Nevertheless, it shows low dimensional accuracy, resolution, and stair-steps effect, it requires post-processing for a smooth finish, and the layer adhesion mechanism makes its parts highly anisotropic (Gao et al. 2015; Kumar et al. 2018; Thompson et al. 2019). In MEX, the selection of the process parameters and a detailed printing plan must be carefully improved to optimize the mechanical characteristics, quality, and surface roughness of the manufactured components (Gonzalez-Gutierrez et al. 2019; Sanchez et al. 2019).

Generative design, implemented recurring to Fusion 360, is the capability of CAD applications to autonomously generate a series of design alternatives given a set of constraints, which can be done without the guidance of an engineer and through artificial intelligence algorithms. It varies from other design processes because it starts at an arbitrary formulation of an initial design concept. This approach should combine the algorithms' critical structures and variables transformed by the algorithms (Cui and Tang 2017). For Tang and Cui, the generative design process is iterated by probing more variables until the users themselves stop it. They proposed a scheme for the generative design application, as shown in [Figure 2](#).

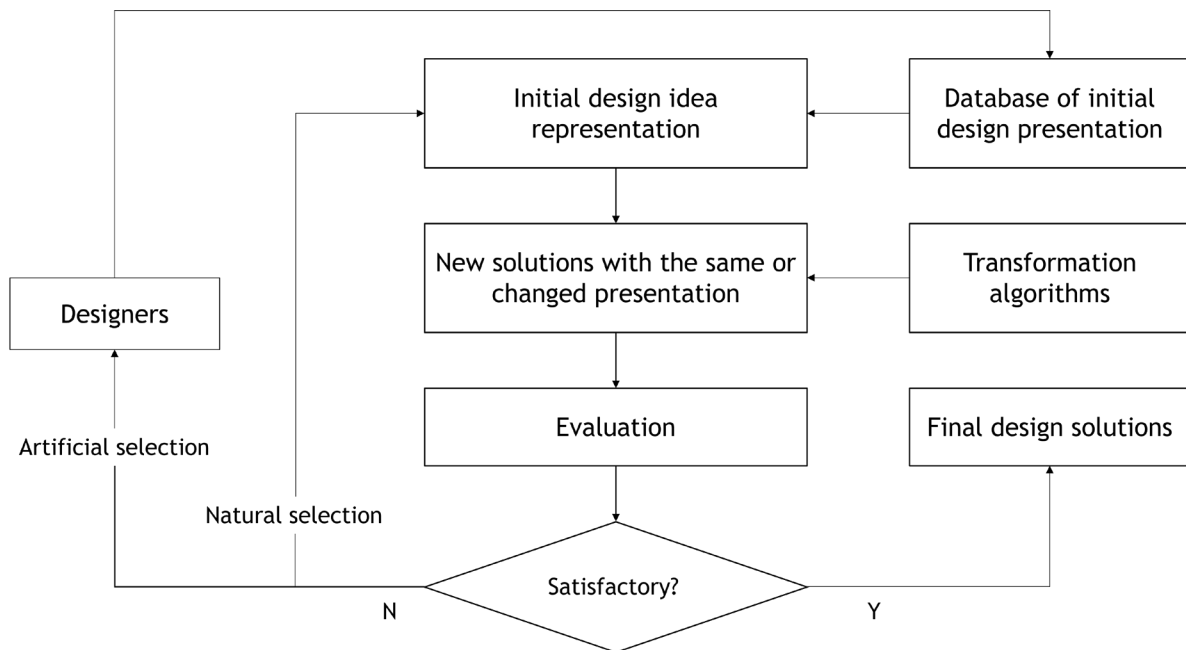


Figure 2: Generative Design Procedure (Cui and Tang 2017).

The generative design process commences with the definition of the purposes and constraints of the project. These include, but are not limited to, design parameters: the product size and geometric dimensions, the permissible loads and operating conditions, the intended weight, the materials, the manufacturing methods, and the cost per unit manufactured. Generative design is a worthwhile process, as it allows the creation and simulation of thousands of designs in short times and the production of highly customized complex shapes (Vuillemot and Huron). The nTopology software is used for DfAM. The selected one for this case is used to optimize the stapler. It combines design for AM (DfAM) and simulation tools, allowing the creation of parts with well-defined functional requirements. The incorporated applicable requirements address and solve the typical conflicts between design and engineering to obtain lightweight components and optimized parts (Gebisa and Lemu 2017; Yang and Zhao 2015).

This work aimed to develop and topologic optimization of a functional stapler by MEX in Inconel 625. The chosen material is an exercise despite excellent protection against corrosion and oxidation. This would not be the material of choice in the industrial development of fasteners. The only way to produce this type of part using a material like Inconel would be for a premium market, where it would be valued not only the premium material but also an elevated level of personalization, specifically developed for the customer in question. The main sights of this work are the development of skills in DfAM and the study of the printed parts. From a market point of view, the component chosen is not supposed to compete with the traditional and cheap polymeric staplers but to play in the high-end market, where uniqueness, customization, and materials nobility are essential.

2. Materials and Methods

2.1. The Inconel 625

The Inconel 625 is a nickel-base solid-solution-strengthened superalloy. It is used in numerous applications in industries that demand custom-made components due to its appealing properties, namely its high corrosion and oxidation resistance in hostile environments, high yield strength, fatigue and creep strength, and good weldability (Vuillemot and Huron). This alloy can resist temperatures from cryogenic up to 1200 °C. The chemical composition of Inconel 625 gives it outstanding properties, and it is presented in [Table 1](#).

Chromium (Cr)	20-23%
Molybdenum (Mo)	8-10%
Iron (Fe)	< 5%
Niobium (Ni)	3.15-4.15%
Cobalt (Co)	< 1%
Manganese (Mn)	< 0.5%
Silicon (Si)	< 0.5%
Aluminum (Al)	< 0.4%
Titanium (Ti)	< 0.4%
Carbon (C)	< 0.1%
Phosphorus (P)	< 0.015%
Sulfur (S)	< 0.015%
Nickel (Ni)	Balance

Table 1: Chemical Composition (in %) of Markforged Inconel 625.

The content of chromium and molybdenum is high, providing good corrosion resistance and strength, at the same time as Fe and Nb potentiate further solid solution strengthening. Aluminum and titanium are added in low percentages to enhance refinement and favor weldability.

The biggest problem with Inconel 625 is the low surface hardness of the annealed condition (0-19 HRC) (Gunen and Kanca 2017) and the difficulty in machining while maintaining good surface integrity (Gong et al. 2020), which can be solved through AM processing. Inconel 625 is an easy alloy to print by MEX and allows the production of functional components.

2.2. Topology Optimization and Manufacturing

In the process of redesigning and optimizing a stapler, the first step was to design a stapler using the Autodesk Fusion 360, using a standard stapler that was acquired and widely available in the market; to enable an accurate design, it was used a caliper, to allow accurate dimensions of the CAD model. This stage was essential once the objective was to take the loader and incorporate it into the housing developed by MEX. The resulting measurement and additional features, the adaptors and springs, were added to the initial model. Figure 3 shows the stapler available in the market and the CAD model designed.



Figure 3: Real Stapler and CAD Model Adapted to Fit the Actual Dimensions.

From this point on, it was possible to start optimizing for AM to obtain the minimum mass and ensure a base and safety factor (SF) of 2. The SF translates the relationship between the yield and the maximum work stress the component must bear. Its function is to cover the differences between real-life factors and the loads and restrictions defined for a simulation. It is not capable of quantifying all parameters related to the systems. The choice of a SF must take into consideration some requirements: material, final cost, service conditions, design, analysis, and processing (Mascarenhas, Ahrens, and Ogliari 2004). For this case, a SF of 2 is

enough to validate the component’s structural integrity. The first component to be developed was the Top Case. However, before moving to the development of AM design, a Static Test in the Simulation module of the software was performed to understand how the component would react in work. The parameters defined are presented in [Table 2](#).

Material	Inconel 625
Constraints	Fix holes for the axis
Load Case	40 N applied onto the Top Case's periphery
Minimum Safety Factor	2
Maximum overhang	45°
Minimum thickness	3 mm

Table 2: Simulation Parameters Used in the Static Simulation Test.

The force used in the load case was based on the force that a medium-size human applied when making a move, as the one applied on a stapler. This deduction was required since any standard for the mechanical properties of a stapler was not found. These parameters will be used in every simulation performed in the Top Case. The results of the Static Test performed in the conventional top case component in the *Simulation Module* of the *Fusion 360* are shown in [Table 3](#). The simulation computes the applied force and respective mechanical behavior for each point within the generated mesh. The given values in [Table 3](#) represent the highest ones obtained.

Parameters	Mass (g)	Min SF	Max stress (MPa)	Max displacement (mm)	Max strain
	229	5.8	110.3	0.074	0.0012

Table 3: Resulting Mechanical Values of the Static Test Performed in the Conventional Top Case Component.

In the development of the actual part, three different components were created. Two of them were conceived using generative design (GD) algorithms with the same parameters described by the Static Test, one with the Generative design module in Autodesk’s software *Fusion 360* and the other with the *nTopology* software. The *nTopology* enables the end-user to optimize the design by facilitating the component development with high-value structures -like lattice, topological optimization, and generative design, reducing engineering bottlenecks when these features are introduced. Using advanced geometry and design data brings diverse generative design toolsets by managing the complexity of advanced manufacturing, with more variations already underlaid in the software, in a shorter time. In [Figure 4](#), the study setup got by using *Fusion 360* is presented. The last component was also developed using *nTopology*, but in this case, it simply added lattices to the conventional part. The selection process and posterior adjustments will be discussed in the next chapter.

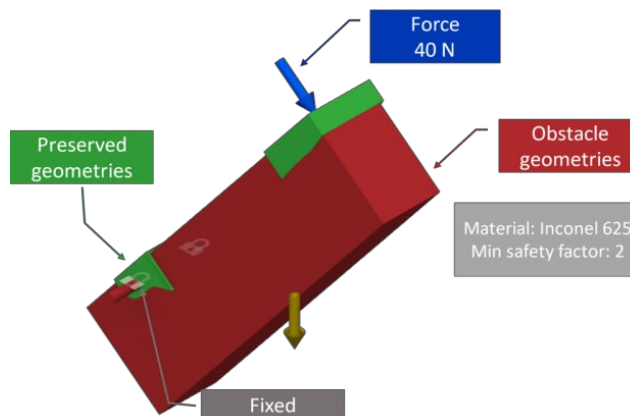


Figure 4: Study Setup, of the Top Case, for Generative Design Simulation Using *Fusion 360*.

Based on the results of the previous study, in the development of the Base Case, an initial static test was performed, and its effects are presented in Table 4. Right after, the generative design simulation in Fusion 360 was initiated.

Parameters	Mass (g)	Min SF	Max stress (MPa)	Max displacement (mm)	Max strain
	114	1.6	403.7	0.056	0.0048

Table 4: Resulting Mechanical Values of the Static Test Performed in the Conventional Base Case Component.

The same material and SF were used in this case. The constrained faces were the holes where the axis will be inserted, and the load case was the parameter signaled in blue in Figure 5. An applied force of 40 N was defined for the top preserved geometry, the spring, and clip housing, based on the pressure applied in the Top Case. The resulting model will be analyzed in the next chapter.

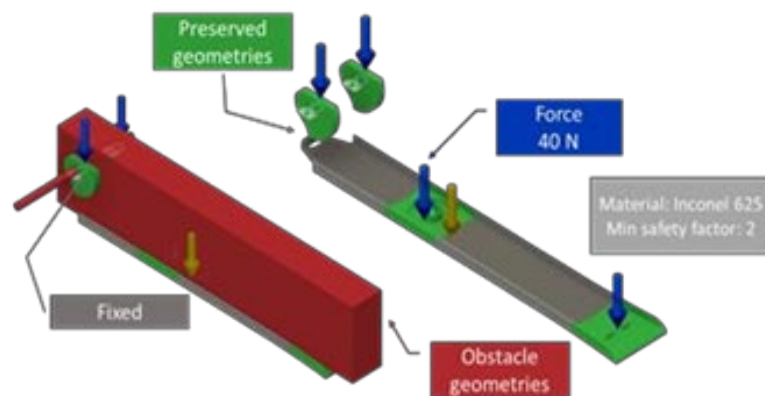


Figure 5: Study Setup, of the Base Case, for Generative Design Simulation Using Fusion 360.

The CAD model was imported to Eiger software for the manufacturing phase, facilitated by Markforged. The best position for printing the stapler, both Top Case and Base Case, was based on simulations. These are derived from the material, furnace types, and printer type - Inconel 625, Sinter-1, and Metal X, respectively, and a post-sintered layer height of 0.125 mm. The infill used in this project was a solid infill with four wall layers – 1.00 mm post-sintered. After that, various orientations were experimented with, finding that the best for Top and Base Cases were the positions presented in Figure 6.

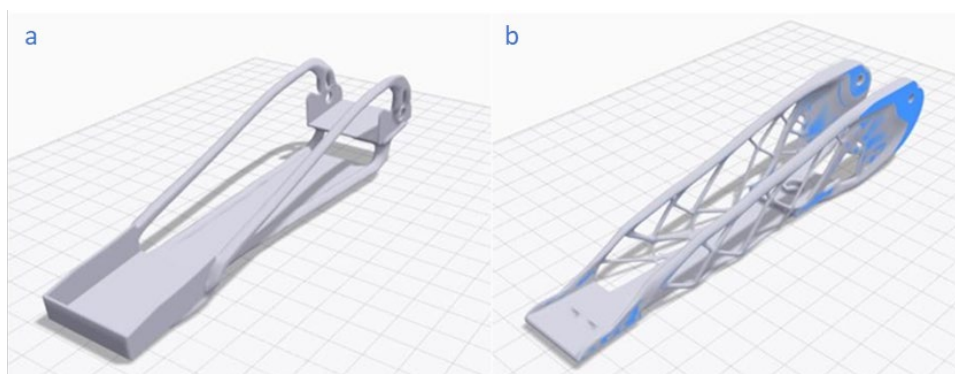


Figure 6: Best Orientations for Printing for the Top Case (a) and the Base Case (b).

The printing orientation for both pieces was chosen based, fundamentally, on the density of required binders, the print time, and the final part mass and metal volume. The software also gives information regarding the material cost, although, in this experiment, which was not relevant, as the goal was the production of a highly customized unique stapler.

In [Figure 7](#), the internal views for both cases of the stapler are displayed. The final part is shown in silver, the binders in purple, the release in orange, and the raft needed for supporting the piece in yellow.

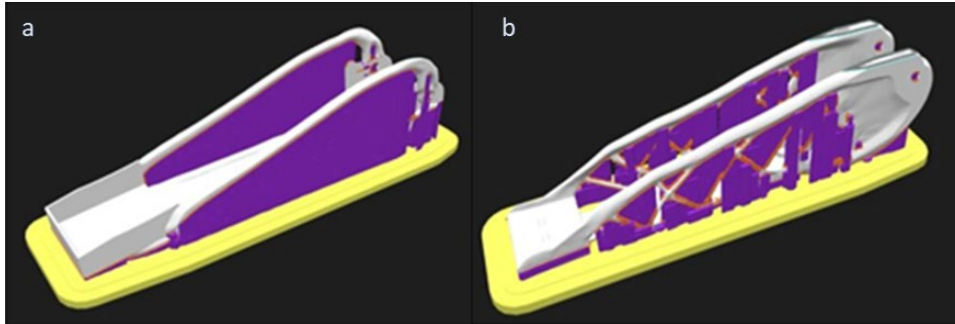


Figure 7: Printing Schemes at Eiger.io (Markforged Software) for the Top Case (a) and the Base Case (b).

After the production of the component layer-by-layer was concluded, the debinding was performed. It was used to remove the ceramic binders from the fabricated pieces, leaving the components very fragile. This fragilization resulted in a breakage of the top part of the stapler, which was not foreseen, as the critical factor was the bottom one due to the mesh implemented.

The broken component was not sintered since it was no longer usable. The bottom part was treated at the conditions automatically defined by Eiger based on the material and geometry printed. The Markforged software does not allow the operator to manipulate the parameters defined by their algorithm. In the end, this piece was problematic, breaking during sinterization.

3. Discussion

3.1. Topology Optimization - Top Case Development

As explained in the procedure, three different versions of a possible outcome for the Top Case were created. The resulting models are shown in [Table 5](#) alongside the results from the corresponding Static Test. Each test for both GD models was conducted in the same program as the component was developed, and it was considered the last iteration.

Type	Generative Design in Fusion 360	Generative Design in nTopology	Lattices Implementation on nTopology
Component Name	GD_FS_SF2	GD_nTop	LT_nTop
Model			
Mass (g)	51	-	184
Min SF	2.5	-	-
Max Stress (MPa)	259.7	-	-
Max Displacement (mm)	0.945	-	0.454
Max Strain	0.0025	-	0.0023

Table 5: Different Optimizations Made and Resulting Mechanical Values of the Static Test.

After obtaining the simulation results, it was clear that there were only two viable options, the components GD_FS_SF2 and LT_nTop. Despite being interesting, the development of the simulation GD_nTop was not a realistic choice. There, and to save time, the model was abandoned, and no further testing was made. The results of the Static Tests conducted in the two best options revealed that the LT_nTop had better mechanical properties (displacement and strain). However, the mass difference of 72% between the two was high to be overlooked. Considering that the lattices added to the model would be challenging to produce by MEX, the component selected was the GD_FS_SF2.

At this point, there was a need to increase the mechanical properties without excessively increasing the mass. Two solutions were found manually by adapting the model to decrease the displacement and repeating the simulation, increasing the SF up to 5. The manual adaptations were made before the simulation, and the results were similar. Table 6 shows the resulting components, respective mechanical values, and percentage deviation from the model from the GD_FS_SF2.



Type	Generative Design in Fusion 360		Generative Design in nTopology	
Component Name	GD_FS_SF2_AD		GD_FS_SF5	
Model				
Mass (g)	64	20%	72	29%
Min SF	3.4	33%	2.6	5%
Max Stress (MPa)	173.3	33%	247.8	5%
Max Displacement (mm)	0.189	80%	0.164	83%
Max Strain	0.0014	44%	0.0028	9%

Table 6: Different Adaptations Made to GD_FS_SF2 and Resulting Mechanical Values of the Static Test Performed in the Conventional Component.

Both adaptations were successful, increasing the minimum SF from 2.5 to 3.4 and 2.6, and reducing the stress and displacement without too big increments in the components' mass. Therefore, a closer look at the displacement and stress must be taken to choose accurately. The displacement is a meaningful property to analyze because it allows the designer to see in which direction the component will be deformed. In Figure 8, the results are associated with the displacement and stress for both components. The GD_FS_SF5 gives a lower displacement, but it is an irregular deformation in two directions - X and Z. On the other hand, the GD_FS_SF2_AD will only deform in the X-direction. This is an advantage seeing how the splatter moves. Considering the yield strength (YS) of the Inconel 625, 207 MPa [16], it can be concluded that the component GD_FS_SF2_AD will be deformed elastically and the GD_FS_SF5 plastically in the hole for the axis (247.8 MPa surpasses the YS). Yet, in the region where the displacement is significant, the deformation will be elastic. After considering all these variables and the mass, the final component was chosen as the last version, GD_FS_SF2_AD.

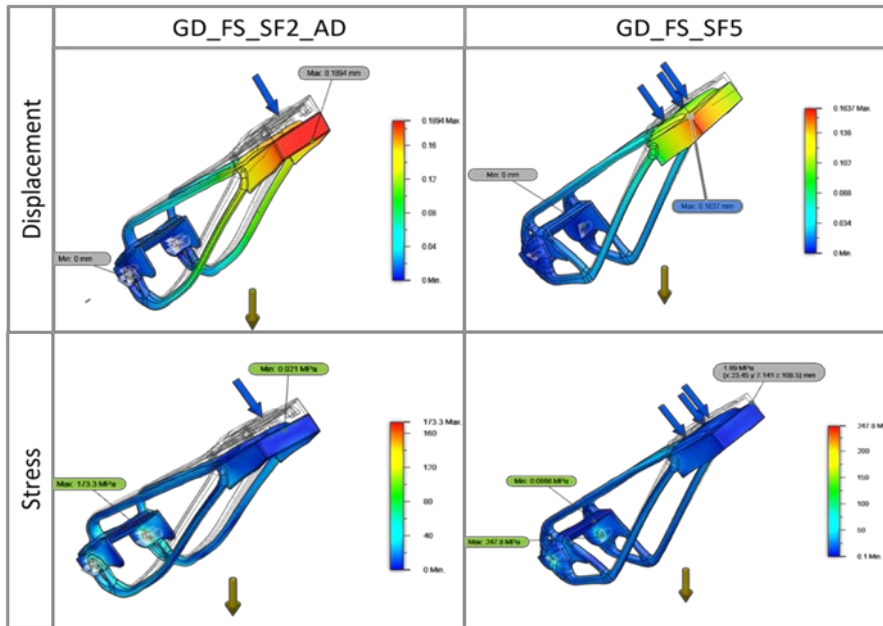


Figure 8: Static Test Simulation Results for the Displacement and Stress Obtained from the Components GD_FS_SF2_AD and GD_FS_SF5.

The best component version had been reached, with a decrease of the mass of 72% compared to the conventional part, supplemented by good mechanical features. In addition, this component does not contain any element impossible to produce by MEX. The more significant obstacle for this design will be the extensive need for supports and the staircase affected by the round surfaces. This last one could be minimized with post-processing.

Nevertheless, since this component is supposed to be a high-end object, customizations are essential. The Inconel is not the material of choice in the industrial development of fasteners. The only way to produce this type of part using a material as the one used in this study, would be for a premium market. There it would be valued as a high-end stapler with an elevated level of personalization, specifically developed for the customer in question. In addition, a surface on the top of the element that allows printing any word or sentence was added to make this an added value piece. It has added the advantage of preventing dust accumulation on the loader. The result of the GD_FS_RP is shown in Figure 9, and the resulting mechanical values of the Static Test are in Table 7.

Parameters	Mass (g)	Min SF	Max stress (MPa)	Max displacement (mm)	Max strain
	76	3.6	179.4	0.0156	0.0014

Table 7: Resulting mechanical values of the Static Test performed in the GD_FS_RP.



Figure 9: Components Wholly Optimized and Ready to Print.

The addition will result in a mass increment of 16% and maximum stress of 3% in the axis's holes surroundings. Nonetheless, the displacement decreases by 17%, a nominal decrease of 0.033 mm. The material addition did not have a significant mechanical value.

3.2. Topology Optimization - Base Case Development

For the development of the Base Case, it was only considered the possibility of generative design with Fusion 360 since it was proved in the previous component that this was more efficient for MEX, presenting a higher mass decrease.

The generative design resulted in 38 iterations, and even though the last one presented a mass of only 37 g, the design was not functional and too challenging to produce by FDM. So, it was considered iteration 22 for further developments, named GD_BC_RP. This iteration was 45% heavier; however, the features were doable by the technique in the study and esthetically more appealing. Both iterations are presented in Figure 10.

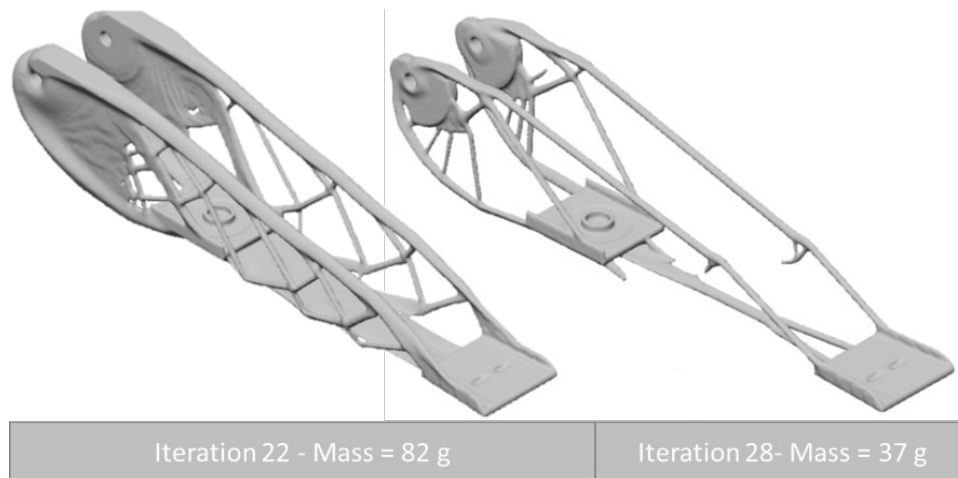


Figure 10: Iterations 22 and 45 Resulting From the GD Simulation of the Base Case.

The next step was to manually adjust some problematic features and conducting a Static Test. The results are shown in Table 8. The findings were outstanding; therefore, no further adaptations to the model were needed, with a decrease of 72% of the initial mass. The component was ready to print.

Parameters	Mass (g)	Min SF	Max stress (MPa)	Max displacement (mm)	Max strain
	85	10.32	62.14	0.0422	6.79e-04

Table 8: Resulting Mechanical Values of the Static Test Performed in the GD_BC_RP.

As can be deduced by the smaller workflow, Base Case took less time to be developed. This happened because, in the previous stage, all the hypotheses were explored, and the acquired knowledge was applied here. Hence, it was possible to increase the productivity of the topology optimization stage highly. At last, the GD_BC_RP was transferred to the nTopology software, where lattices in the massive part of the component were added to decrease the mass and increase the aesthetic value without compromising the mechanical properties. The resulting component is shown in Figure 11. As mentioned before, lattices are not very suitable for the AM technique in the study, so this experiment was performed for future research with different AM processes, namely Laser Powder Bed Fusion.



Figure 11: GD_BC_RP With Lattices Added in nTopology.

3.3. Assembly Test

The last phase determined if the components could be assembled or if quotas got incompatible during the re-modeling. In a first test, it was recognized that the pieces could not fit together for just a few millimeters because of the material added to the trailing edge of the Base Case. Nevertheless, the additional material was removed with the help of a cutting plane. This operation made the mass of GD_BC_RP decrease to 74 g, corresponding to a reduction of 9 g in the total weight; however, the mechanical properties presented in Table 8 remained constant. After that, the components assembled perfectly together, as seen in Figure 12. The geometry is overly complex and requires additional working near the capacity limit of the machine regarding feature limits. One of the core objectives of this investigation research was to be disruptive and check if it is possible to produce such a complex geometry recurring to MEX, including small diameters like the ones experimented.



Figure 12: Photorealistic Image of the Assembled Components
GD_FS_RP and GD_BC_RP.

The resulting components of the last step of the parts modeling phase are the GD_FS_RP and the GD_BC_RP, which were transferred to the Markforged software, Eiger.

3.4. Manufacturing

As discussed previously, Eiger was used to choose the best printing position for both stapler components, and it was possible to predict a printed mass of 303.56 g for the top part and 191.31 g for the base. For the top, 75% of the weight referred to supports, while for the base, the value was a little lower but still significant, 58%. A new weighing was done to compare the simulated and the obtained components. After the fabrication, it was verified that the printed

mass had been 287.1 g and 178.1 g for the top and the bottom, considering the respective rafts, respectively. A significant mass deviation of 5.73% for the top and 7% for the bottom component of the stapler was denoted. This deviation is justified by the reactions that occur during the print that affect the material integrity, namely its density, which will influence the final weight.

3.5. Printed component evaluation

The resulting printed components were not found to be the expected, even considering the complex geometries imposed and the tolerances of the machine. After sintering, there was a layer height of 0.125 mm, so the machine was anticipated to be capable of producing them.

The Top Case component broke down in the center after the debinding treatment, which was unexpected. However, it can be attributed to the fact that part of the base material was glued to it when removing the parts from the printer constituent, resulting in several fractures after the washing stage. This phenomenon could be explained by damp material and the need for print bed maintenance. Another justification is that it may have been due to the failure of the supports built underneath the broken area. This failure may be related to the release of the binders from the bed where they were born or these not being resistant enough to reinforce the structure. Reasons for this can be the leveling of the individual bed, the material humidity, the need for maintenance, or the geometry and orientation of the workpiece. Another parameter that could have helped the destruction was the geometry and small features of the model. Namely, the sheet contained the acronym DEMM, which only had a surface embossment of 1.5 mm.

For the Base Case, the structure could not resist the sintering phase. In contrast to what happened in the other component, the phenomenon is efficiently explained by the diameters used in the lattice-like structures, with a minimum diameter of 0.89 mm. These were too small to sustain the volume variations during the part sintering and cooling, resulting in its collapse.



Figure 13: CAD Model With the Areas to Rework Marked and Falling Printed Parts.

Specific model adaptations should be considered in some areas; these sections are highlighted in [Figure 13](#) and were defined by studying the resulting parts. The solution was to increase the minimum feature thickness for each case to 2.5 mm and, in the case of the Top Cases lattice-like structure, increase the diameter to 2.5 mm. Both components were not functional, and the procedures ended. However, in an ideal situation, the parts would need post-processing. After re-printing the components, some post-processing must be done. The first step would be to remove the supports and perform a polishing or electrochemical polishing on the rougher and more pronounced surfaces. Inconel parts produced by SLM result in a smoother and shinier surface and a diminished stair-step effect (Jain et al. 2021).

4. Conclusions

This work reconfirmed the pertinence of optimized components and the feasibility of their production thru AM in general by redesigning an everyday tool.

Despite being quite challenging, the design and optimization modeling step demonstrated reliable results, and the material is chosen for its noble properties, Inconel 625, proved to be an adequate solution. However, it could not be the best considering the failure during the print. The topology optimization showed outstanding results, mainly mass reduction without properties damage. With the workflow followed, it was possible to decrease the Top Case and Base Case masses by 70% and 30%, associated with a displacement of 0.156 mm and 0.0422 mm, respectively. For the stapler, it was possible to reduce the mass by 54%.

The goal of getting successful results working on the threshold limit of the machine was not materialized since there were some embrittlement problems, resulting in the fracture of both components - the Top Case after washing and the Base Case after sintering. This problem will require redesigning top and base support cases to enable a suitable part produced through MEX. Extrusion processes require increased dimensions compared to other AM processes like laser powder bed fusion (LPBF), and it would be interesting to evaluate these designs.

References

- ASTM. 2019. ISO/ASTM52921-13(2019), Standard Terminology for Additive Manufacturing—Coordinate Systems and Test Methodologies. West Conshohocken, PA: ASTM International. <https://doi.org/10.1520/ISOASTM52921-13R19>.
- Costa, José, Elsa Sequeiros, Maria Teresa Vieira, e Manuel Vieira. 2021. "Additive Manufacturing: Material Extrusion of Metallic Parts". *U.Porto Journal of Engineering* 7 (3): 53–69. https://doi.org/10.24840/2183-6493_007.003_0005.
- Cui, Jia, e Ming Xi Tang. 2017. "Towards Generative Systems for Supporting Product Design". *International Journal of Design Engineering* 7 (1): 1. <https://doi.org/10.1504/IJDE.2017.085639>.
- Gao, Wei, Yunbo Zhang, Devarajan Ramanujan, Karthik Ramani, Yong Chen, Christopher B. Williams, Charlie C.L. Wang, Yung C. Shin, Song Zhang, e Pablo D. Zavattieri. 2015. "The Status, Challenges, and Future of Additive Manufacturing in Engineering". *Computer-Aided Design* 69 (dezembro): 65–89. <https://doi.org/10.1016/j.cad.2015.04.001>.
- Gebisa, A.W., e H.G. Lemu. 2017. "Design for Manufacturing to Design for Additive Manufacturing: Analysis of Implications for Design Optimality and Product Sustainability". *Procedia Manufacturing* 13: 724–31. <https://doi.org/10.1016/j.promfg.2017.09.120>.
- Gong, Le, Rachele Bertolini, Andrea Ghiotti, Ning He, e Stefania Bruschi. 2020. "Sustainable Turning of Inconel 718 Nickel Alloy Using MQL Strategy Based on Graphene Nanofluids". *The International Journal of Advanced Manufacturing Technology* 108 (9–10): 3159–74. <https://doi.org/10.1007/s00170-020-05626-x>.
- Gonzalez-Gutierrez, Joamin, Florian Arbeiter, Thomas Schlauf, Christian Kukla, e Clemens Holzer. 2019. "Tensile Properties of Sintered 17-4PH Stainless Steel Fabricated by Material Extrusion Additive Manufacturing". *Materials Letters* 248 (agosto): 165–68. <https://doi.org/10.1016/j.matlet.2019.04.024>.
- Gonzalez-Gutierrez, Joamin, Santiago Cano, Stephan Schuschnigg, Christian Kukla, Janak Sapkota, e Clemens Holzer. 2018. "Additive Manufacturing of Metallic and Ceramic Components by the Material Extrusion of Highly-Filled Polymers: A Review and Future Perspectives". *Materials* 11 (5): 840. <https://doi.org/10.3390/ma11050840>.

- Gunen, Ali, e Erdogan Kanca. 2017. "Microstructure and Mechanical Properties of Borided Inconel 625 Superalloy". *Matéria (Rio de Janeiro)* 22 (2). <https://doi.org/10.1590/s1517-707620170002.0161>.
- Jain, Srishti, James Hyder, Mike Corliss, e Wayne NP Hung. 2021. "Electrochemical Polishing of Extruded and Laser Powder-Bed-Fused Inconel 718". *International Journal of Engineering Materials and Manufacture* 6 (4): 284–98. <https://doi.org/10.26776/ijemm.06.04.2021.04>.
- Kumar, Narendra, Prashant Kumar Jain, Puneet Tandon, e Pulak M. Pandey. 2018. "Extrusion-Based Additive Manufacturing Process for Producing Flexible Parts". *Journal of the Brazilian Society of Mechanical Sciences and Engineering* 40 (3): 143. <https://doi.org/10.1007/s40430-018-1068-x>.
- Mascarenhas, W.N., C.H. Ahrens, e A. Ogliari. 2004. "Design Criteria and Safety Factors for Plastic Components Design". *Materials & Design* 25 (3): 257–61. <https://doi.org/10.1016/j.matdes.2003.10.003>.
- Sanchez, Larissa Cristina, Cesar Augusto Gonçalves Beatrice, Cybele Lotti, Juliano Marini, Sílvia Helena Prado Bettini, e Lidiane Cristina Costa. 2019. "Rheological Approach for an Additive Manufacturing Printer Based on Material Extrusion". *The International Journal of Advanced Manufacturing Technology* 105 (5–6): 2403–14. <https://doi.org/10.1007/s00170-019-04376-9>.
- Singh, Sunpreet, Seeram Ramakrishna, e Rupinder Singh. 2017. "Material Issues in Additive Manufacturing: A Review". *Journal of Manufacturing Processes* 25 (janeiro): 185–200. <https://doi.org/10.1016/j.jmapro.2016.11.006>.
- Thompson, Yvonne, Joamin Gonzalez-Gutierrez, Christian Kukla, e Peter Felfer. 2019. "Fused Filament Fabrication, Debinding and Sintering as a Low Cost Additive Manufacturing Method of 316L Stainless Steel". *Additive Manufacturing* 30 (dezembro): 100861. <https://doi.org/10.1016/j.addma.2019.100861>.
- Tofail, Syed A.M., Elias P. Koumoulos, Amit Bandyopadhyay, Susmita Bose, Lisa O'Donoghue, e Costas Charitidis. 2018. "Additive Manufacturing: Scientific and Technological Challenges, Market Uptake and Opportunities". *Materials Today* 21 (1): 22–37. <https://doi.org/10.1016/j.mattod.2017.07.001>.
- Vuillemot, Romain, e Samuel Huron. 2017. "Glitch e s as a Generative Design Process". Em 2017 IEEE VIS Arts Program (VISAP), 1–6. Phoenix, AZ: IEEE. <https://doi.org/10.1109/VISAP.2017.8282377>.
- Yang, Sheng, e Yaoyao Fiona Zhao. 2015. "Additive Manufacturing-Enabled Design Theory and Methodology: A Critical Review". *The International Journal of Advanced Manufacturing Technology* 80 (1–4): 327–42. <https://doi.org/10.1007/s00170-015-6994-5>.